remote sensing

MDPI

Article

Reconstruction of the Water Cultivation Paleoenvironment Dating Back to the Han and Tang Dynasties Surrounding the Yangguan Frontier Pass Using X- and L-Band SAR Data

Xiaokun Zhu [1,2,3], Fulong Chen [1,4,*] and Huadong Guo [1,4]

1 Key Laboratory of Digital Earth Science, Institute of Remote Sensing and Digital Earth, Chinese Academy of Sciences, Beijing 100094, China; zhuxk@radi.ac.cn (X.Z.); guohd@radi.ac.cn (H.G.)
2 University of Chinese Academy of Sciences, Beijing 100049, China
3 Beijing Institute of Surveying and Mapping, Beijing 100038, China
4 International Centre on Space Technologies for Natural and Cultural Heritage under the Auspice of UNESCO, Beijing 100094, China
* Correspondence: chenfl@radi.ac.cn; Tel.: +86-10-82178198

Received: 31 July 2018; Accepted: 20 September 2018; Published: 25 September 2018

check for updates

Abstract: Supported by a shallow groundwater wetland ecosystem, the Nanhu oasis, which is the location of the Yangguan frontier pass, represents an important supply and defence station for the ancient Silk Road. The reconstruction of the evolution of the water cultivation environment is helpful for archaeological surveys and the protection of this well-known heritage site. This study proposes a workflow for reconstructing the water cultivation paleoenvironment-based primarily on X- and L-band spaceborne synthetic aperture radar (SAR) data. First, TerraSAR-X/TanDEM-X (TSX/TDX)-generated Digital Elevation Model (DEM) data were used for microrelief analyses, including a watershed analysis and drainage network extraction. Several dried-up paleochannels and the range of the Daze (a wetland dating back to the Tang Dynasty (618–907 A.D.)) were identified. Second, based on the hydrological sensitivity analysis of the multi-temporal L-band SAR data, arid land vegetation accompanying the emergence of groundwater was extracted to locate ancient arable areas using backscattering and coherence characteristics. Finally, reconstruction of the water cultivation paleoenvironment surrounding the Nanhu oasis dating back to the Han and Tang dynasties (202 B.C.–907 A.D.) was performed, referring to historical documents. New discoveries were validated by field campaigns, and the results of the SAR archaeological investigations conducted in this study indicated that the ancient arable area in the Nanhu oasis was nearly double the current dimensions.

Keywords: spaceborne SAR; Nanhu oasis; Yangguan frontier pass; water cultivation paleoenvironment; Han and Tang dynasties

1. Introduction

The Nanhu oasis, where the famous Yangguan frontier pass was allegedly located, is the westernmost oasis of the Hexi Corridor in China. It represents the starting point of the southern route of the Silk Road through the Kumtag Desert to the ancient cities of Puchanghai (now Lop Nor) and Shanshan [1]. Serving as the most important supply station in the region, the Nanhu oasis has a unique geographical environment involving a shallow groundwater wetland ecosystem with nearly 200 springs and wetlands in an extremely arid desert region. The oasis is surrounded by vast uninhabited deserts and the Gobi Desert, whereas the oasis itself features abundant underground spring water resources, making the Nanhu oasis the most liveable area within the deserts. This region has acted as the westernmost borderland since the Western Han Dynasty (202 B.C.–8 A.D.), and population migration has represented an important strategy for exploiting the arable areas in the oasis and stabilizing frontier defences in this region. Relying on abundant groundwater resources from the Dang River, large-scale military farms and pastures in the Nanhu oasis were developed to guarantee frontier defence and a food supply. According to Stein's statistics, all streams, including surface water and groundwater, produce a total flow rate of more than 80 cubic feet per second, which could meet the needs of a farming area thirty times larger than that observed in the 1900s [2]. The famous Yangguan frontier pass established during the Western Han Dynasty (202 B.C.–8 A.D.) was the primary means of entry to the western regions. The pass was ultimately abandoned with environmental degradation after the Song Dynasty (960–1279 A.D.); large areas of arable land and farms for defence were also abandoned. Currently, although some areas have been preserved and cultivated, numerous arable areas are buried by sand [2]. The locations of both the Yangguan frontier pass and the large-scale farming areas remain a mystery. Therefore, a systemic reconstruction of the water cultivation paleoenvironment of the Nanhu oasis may provide a reference for archaeological surveys and a better understanding of the heritage site.

The Nanhu oasis is currently surrounded by the Yangguan National Natural Reserve in Dunhuang, which was established on 4 July 1994 [3]. Prior research has mainly focused on Reserve protection [4,5], environmental monitoring and protection [6,7], and the endangered animals, plants, and the biodiversity in the region [8–10]. Research on the water environment of the Nanhu oasis has mainly concentrated on the reserve's land use changes [11] and wetland distribution and degradation [12,13]. From an archaeological perspective, the extremely arid desert environment of the Nanhu oasis has helped preserve the ancient canals, walls, trails, and ruins. The Great Wall, beacon towers, tombs, and the ancient city of Shouchang [14] in the Nanhu oasis were discovered through archaeological fieldwork in the 1900s and can be traced back to the Han and Tang dynasties (202 B.C.–907 A.D.). For the reconstruction of the water cultivation paleoenvironment, most research has relied on archaeological surveys and historical document analysis [1,15]. In the 2000s, large areas of abandoned ridges and farmlands were found by an archaeological survey in Gudongtan [16], west of the currently cultivated area, indicating the presence of arable and liveable paleoenvironments beyond the extent of the modern Nanhu oasis. Research on the quantitative reconstruction of the water cultivation paleoenvironment is limited, and additional quantitative, historical, and spatial-temporal environmental reconstructions and analyses are, therefore, needed to facilitate research and protection of this heritage site.

Considering that the Nanhu oasis topography was formed by geological factors and has changed little since the Han and Tang dynasties (202 B.C.–907 A.D.), the Nanhu paleoenvironment can be reconstructed using the current topography and features, including groundwater and arable lands. The Institute of Remote Sensing and Digital Earth, the Gansu Province Cultural Relic Institute of Archaeology, and the Dunhuang Museum collaborated to locate the sites of the Yangguan frontier pass and the Duwei mansion by using remote sensing, geophysical methods and archaeological field surveys. Reconstructing the water cultivation paleoenvironment of the oasis via spaceborne synthetic aperture radar (SAR) data was one of these tasks.

Remote sensing data, including optical and radar images, have been widely applied in archaeology. Spaceborne SAR images have contributed to locating undiscovered archaeological sites because such data sets are relatively unaffected by weather and clouds [17–20]. Multi-frequency spaceborne radar imaging provides a new tool for archaeological survey [21]. McCauley et al. applied penetrating L-band radar data to detect the paleochannels and Great Wall in an inland arid desert area that is similar to the surroundings of the Nanhu oasis [22,23]. High-resolution X-band SAR data have been used to extract Digital Elevation Model (DEM) data [24] and detect and monitor deformation of a heritage site [25]. Data from L-band Phased Array Synthetic Aperture Radar (PALSAR-1/2) has been effectively applied to detect paleo-rivers, locate the ruins of ancient cities and reconstruct such features currently covered by sand or vegetation [26,27]. In this study, considering the characteristics of the terrain surface and the water cultivation paleoenvironment of the Nanhu oasis, a new workflow was designed to extract the ancient drainage network and then to reconstruct the ancient arable lands using both X- and L-band spaceborne SAR data.

2. Study Area, Materials and Methods

2.1. Study Area

As shown in Figure 1, the Nanhu oasis study area is located in the town of Yangguan, Gansu Province, China, and is surrounded by the Yangguan National Nature Reserve. The Dunhuang West Lake National Nature Reserve and Kumtag Desert are located to the west, the Dang River reservoir is located to the east, Aksay Kazak Autonomous County is located to the south, and the Yumen frontier pass is located to the north. The oasis has a geographical extent of 39°39′N-40°05′N and 93°53′E-94°17′E. The whole area is located on the eastern side of the Tarim plate, which is bounded by the North Altyn tectonic belt and the Yinshan-Tianshan tectonic belt [28]. The traces of the Dang River alluvial flow form a fan extending to the Shule River in the basin, where the beacon towers and the northern extension of the Great Wall were built in the Han Dynasty (202 B.C.–220 A.D.). The current distribution (southwest-northeast zone) of the cultivated area is consistent with the drainage network distribution formed by the alluvial runoff in the oasis.

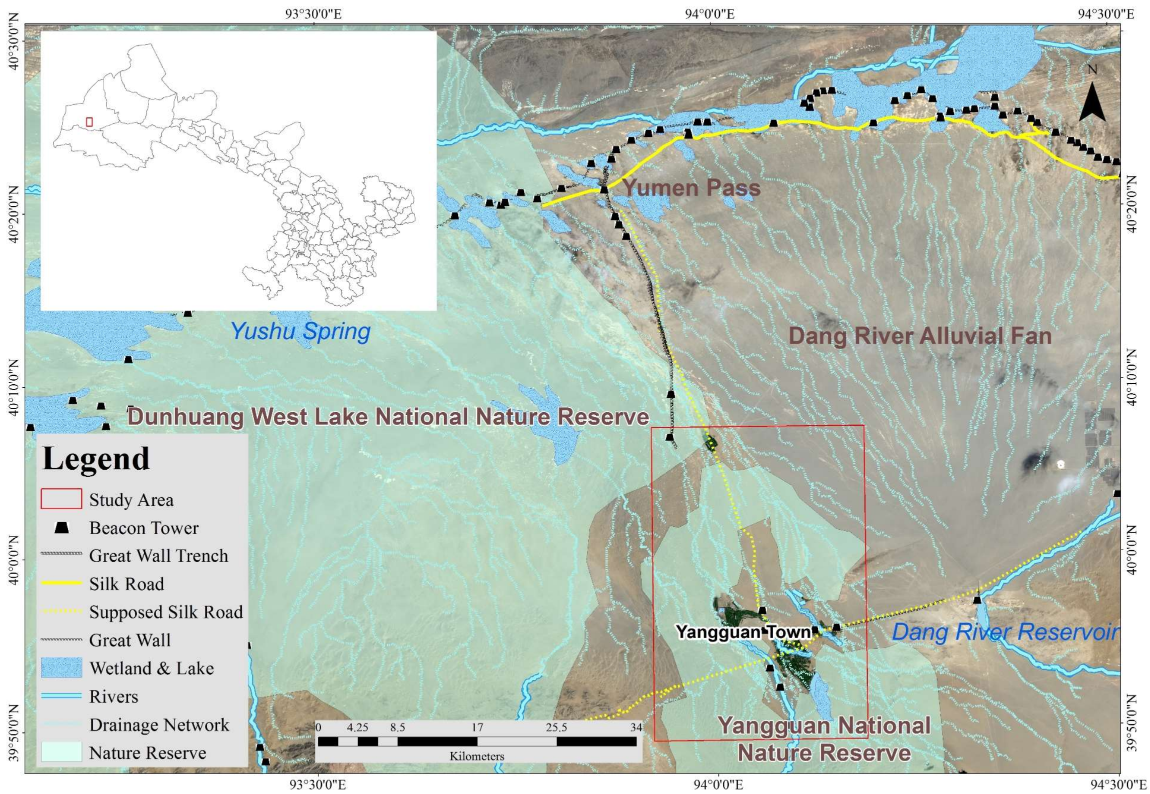

Figure 1. Location of the Nanhu oasis study area is outlined by the red rectangle. The study area is located in the town of Yangguan in the Gansu Province in China (the rectangular box in the upper left part), stretches west to the Dang River alluvial fan, and is surrounded by the Yangguan National Nature Reserve and the Dunhuang West Lake National Nature Reserve, with the famous heritage sites of the Ancient Silk Road and the Han Dynasty beacon towers.

2.2. Materials

2.2.1. Spaceborne SAR Data

The spaceborne SAR data, i.e., two frames of X-band TerraSAR-X/TanDEM-X (TSX/TDX) data covering 4022.36 km^2 and six frames of L-band PALSAR-1 archived data covering 4040.70 km^2, were acquired and are shown in Figure 2. The solid red line, dotted line and black rectangular frames with faint lines represent the coverage ranges of the PALSAR-1 sequential images, the TSX/TDX interference pair, and the study area, respectively.

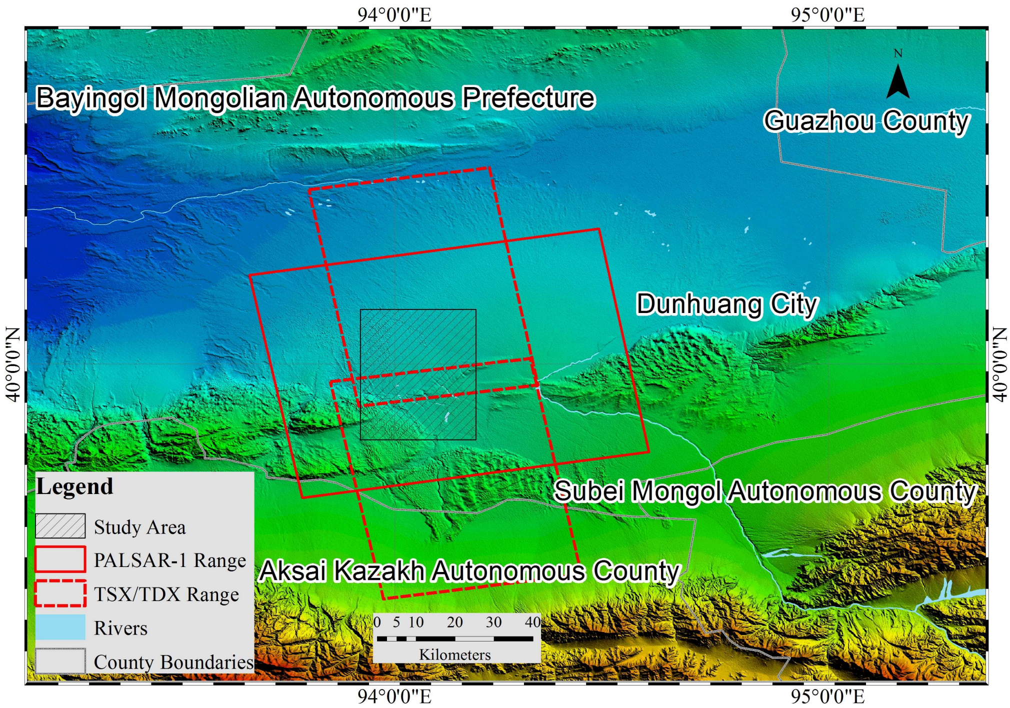

Figure 2. Distribution of the SAR images in the study area. Six frames of PALSAR-1 archived time-series data (rectangle with solid red outline) and two frames of TSX/TDX data (rectangles with dotted red line) covering the entire Nanhu oasis study area (black rectangular frame with faint lines).

The Advanced Land Observing Satellite (ALOS) carrying both optical sensors and L-band PALSAR-1 was successfully launched by the Japanese Aerospace Exploration Agency (JAXA) in January 2006. PALSAR-1 was a phased array SAR providing high resolution (10 m) imagery with variable incidence angle (8 to 60°) and a radiometric accuracy of better than 1 dB [27]. In this study, the time-series PALSAR-1 images were acquired using the following format: JAXA FBS/FBD 1.1, HH polarization, and ascending mode. Six sequential scenes were acquired on 28 June 2007, 30 March 2008, 30 September 2008, 31 December 2008, 6 October 2010 and 21 February 2011. By referring to China's surface international exchange station's daily climate dataset on China's meteorological data website [29], we found that precipitation had occurred within five days prior to the data collection of the images acquired on 28 June 2007, 30 March 2008 and 31 December 2008, whereas precipitation was not observed for the other three dates. Using these time-series data, we can determine changes due to the moisture and permittivity anomalies, which is conducive to identifying different objects.

The TSX/TDX is an X-band radar constellation and a high-resolution interferometric SAR mission of the German Aerospace Centre DLR in conjunction with its partners EADS Astrium GmbH and Infoterra GmbH in a public-private partnership (PPP) consortium. The mission is based on two radar satellites, including TerraSAR-X and TanDEM-X, flying in close formation to achieve the desired interferometric baselines in a highly reconfigurable constellation. TerraSAR-X was launched in June

2007, and TanDEM-X was launched in June 2010. The primary goal of the innovative TSX/TDX constellation is the generation of a global, consistent, timely and high-precision DEM; without the use of ground control points (GCPs), the accuracy can reach 2 m, and the plane error is less than 12 m [30,31]. In this study, 2 Coregistered Angle-look Slant-range Complex (CoSSC) scenes of the TSX/TDX image data were acquired with HH polarization and an ascending 3-m StripMap imaging mode on 19 July 2010 and 19 August 2011.

2.2.2. Reference Visible/Infrared (VIR) Data

The Gaofen-2 satellite was designed and developed by China Academy of Space Technology (CAST). It is a VIR satellite launched in August 2014 with the capable of collecting satellite imagery with a GSD (Ground Sampling Distance) of 0.8 m panchromatic and 3.2 m multispectral bands on a swath of 45 km [32]. The Landsat 8 satellite, as one satellite of the Landsat project, images the entire Earth every 16 days in an 8-day offset from Landsat 7. It carries two push-broom instruments: The Operational Land Imager (OLI) and the Thermal Infrared Sensor (TIRS) [33]. Key Hole (KH) is the designation for a series of American optical reconnaissance satellites, and KH images can be used as important historical materials [34]. One scene of the Gaofen-2 satellite images and one scene of Landsat 8 OLI images with 9 spectral bands were acquired on 23 September 2017 and 23 June 2016 and used as base maps for the data analysis and field investigation. Two scenes of KH archived images acquired in 1976 were geocoded and mosaicked. The resolution of the panchromatic and multi-spectral bands of the Gaofen-2 and Landsat 8 OLI images were 0.8 m and 3.2 m, and 15 m and 60 m, respectively. Data fusion was performed for both data types. True colour band combinations of 321 and 432 were selected for image recognition and information extraction, especially for the interpretation of the vegetation, abandoned channels, dried-up watercourses and ditches in the farmlands.

2.2.3. The Shuttle Radar Topography Mission (SRTM) Data

The SRTM produces the global terrain and is implemented by the U.S. Space Agency (NASA) and the Department of Defense, the National Imagery and Mapping Agency (NIMA), and the German and Italian space agencies. It consisted of a especially modified L-band radar system that flew on board the Space Shuttle Endeavour during a 11-day mission in February 2000 and obtained DEM on a near-global scale from 56°S to 60°N. The new version of the SRTM data (V4.1) covering the entire oasis at 30-m resolution [35] was downloaded for the large-area watershed analysis and as the terrain reference for the TSX/TDX interferometry.

2.3. Method

Considering that the Nanhu oasis topography formed by geological factors has not changed substantially between the Han and Tang dynasties (202 B.C.–907 A.D.) and the present, the drainage network extracted from the terrain surface provided the base map of the paleo-river network. The DEM extracted from the X-band TSX/TDX data with the watershed analysis and drainage network extraction provided the target areas for the dried-up watercourses. An edge detection algorithm was used to calculate the extents of the dried-up watercourses. With the L-band SAR time-series data, filtering and interference enhancement are helpful for reducing seasonal influences and extracting weak information from the phase and intensity anomalies, which form the target areas for the arable lands. A workflow for the extraction of the archaeological water cultivation information from the X-band and L-band spaceborne SAR data was developed; the flowchart is shown in Figure 3.

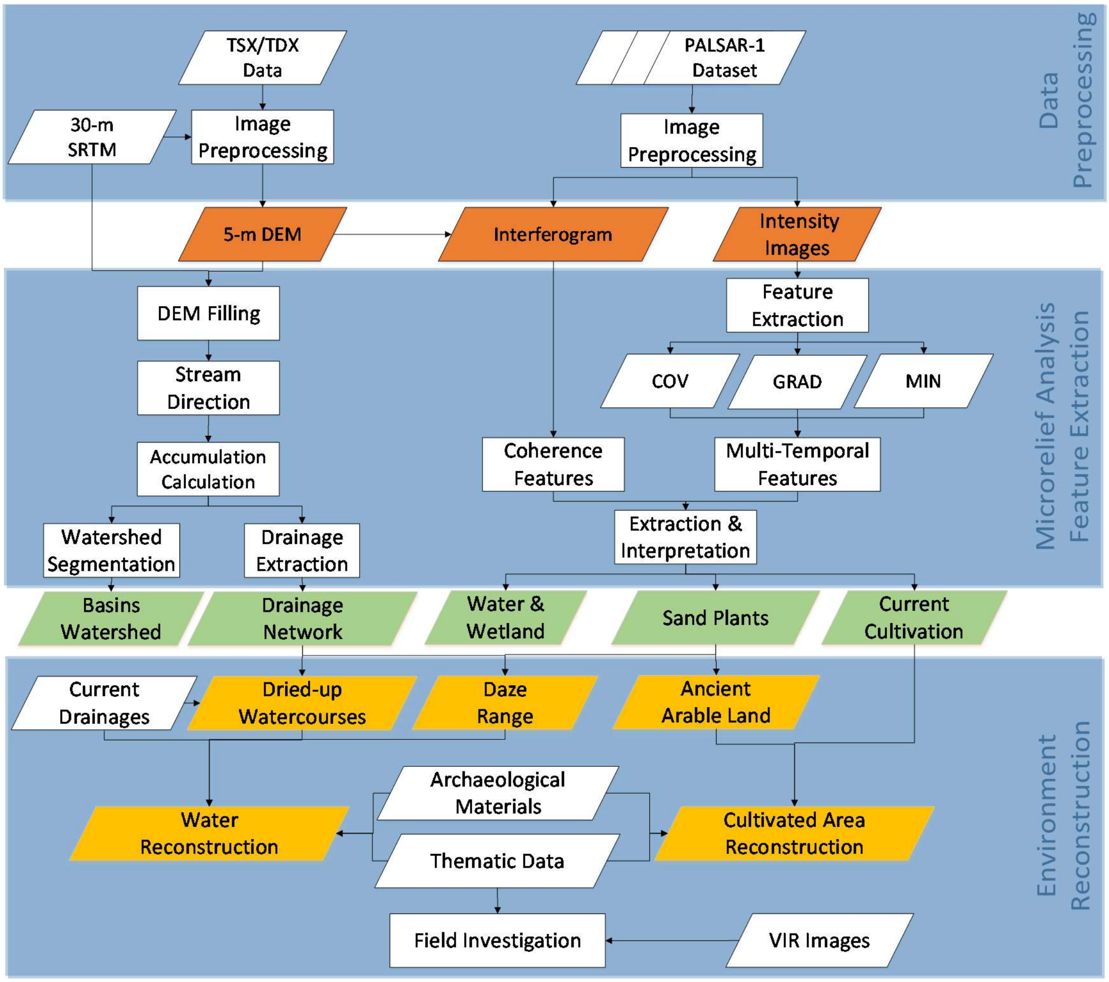

Figure 3. Flowchart of the three main steps: data preprocessing, microrelief analysis and feature extraction, and reconstruction of the water cultivation paleoenvironment. The orange parallelograms, green parallelograms and yellow parallelograms represent the outcomes of the three processing steps.

2.3.1. Data Preprocessing

Data importation and image registration were conducted for both the time-series PALSAR-1 dataset and the TSX/TDX images in the Environment for Visualizing Images (ENVI 5.3) SARScape 5.2.1 software developed by the Swiss company Sarmap. Phase (elevation) and time-series intensity information were obtained through interference (unwrapping) and multi-look filtering to prepare the data for subsequent information extraction and analysis. The sequence of the steps was as follows.

1 TSX/TDX data preprocessing and high-precision DEM extraction

The stripmap TSX/TDX pairs were imported to generate the Single-Look Complex (SLC) data. Image registration, interference, flat-earth phase removal, filtering, phase unwrapping, and geocoding to the final DEM (referred to hereafter as the TDX DEM) were conducted with the 30-m SRTM data. The two extracted TDX DEM datasets were mosaicked. Interpolation of the TDX DEM and SRTM DEM was used for the "no value" areas [36]. The plane Root Mean Square (RMS) error was $\pm$ 1.2 m for geocoding using the GCPs selected from the Gaofen-2 images, and the average height difference between the TDX DEM and the SRTM DEM was 0.9 m and the standard deviation was 3.3 m.

2 PALSAR-1 data preprocessing to obtain time-series intensity images and coherence images [37]

The L-band PALSAR-1 data were preprocessed to obtain the time-series intensity images using image registration, multi-look filtering, and radiation calibration. The TDX DEM results were introduced to generate differential interference results after removing the terrain phase component.

2.3.2. Microrelief Analysis and Feature Extraction

1 Watershed analysis and drainage network extraction based on the SRTM DEM and TDX DEM

The microrelief analysis included a watershed analysis and drainage network extraction. The drainage network extracted from the terrain surface was the source of the paleo-river network. The ArcHydro tool in ArcGIS 10.2 software developed by the Environmental Systems Research Institute (ESRI) was used to extract the watershed and drainage network from the SRTM and TDX DEM data. The maximum distance drop algorithm was used to calculate the depths of flow and depressions in eight directions. The lowest elevation of each contributing area and the height of the outlet of the depression were used to fill the DEM depression areas. In the case of no-depression DEMs, after a comparison with the current thematic map, a threshold was set to extract the drainage network. Flow calculations were conducted for the downstream and upstream directions. The Strahler algorithm was used to acquire the drainage network with six orders, and the watershed segmentation was conducted for each flow distribution [38,39]. The results were compared with the current drainage network and the targeted dried-up watercourses were extracted. Canny edge detection was performed to extract the ranges of the dried-up watercourses and wadis.

2 Feature extraction using the backscattering and coherence characteristics of the time-series PALSAR-1 data

Normally, the state and distribution of arid land vegetation change as the precipitation and groundwater levels change. When the groundwater level depth is between 1 m and 10 m, the results mainly depend on the groundwater level. Therefore, although a portion of the ancient arable area supported by groundwater is covered by sand, the state of the vegetation growth reflects the soil moisture and a clear relationship is observed between the vegetation and the groundwater levels in the study area. The potential arable area can be detected via an analysis of the distribution of the water, wetland and arid land vegetation. The obtained PALSAR-1 data cover different periods with varying surface temperatures and precipitation levels, which is helpful for identifying arid land vegetation from other objects. For the time-series PALSAR-1 intensity data, the coefficient of variation (*COV*), the minimum value (Minimum, *MIN*), and the gradient (Gradient, *GRAD*) were extracted as follows:

$$COV_{i,j} = \frac{STD}{MEAN} = [\sum_{k=1}^{n}\left(x_{i,j,k} - \overline{x_{i,j}}\right)^2/(n-1)]/(\sum_{k=1}^{n} x_{i,j,k}/n)$$
$$COVi,j = \frac{STD}{MEAN} = \sqrt{\frac{\sum_{k=1}^{n}(x_{i,j,k} - \overline{x_{i,j}})^2}{n-1}}/(\frac{\sum_{k=1}^{n} x_{i,j,k}}{n}) \quad (1)$$

$$MIN_{i,j} = \left\{x_{i,j,1}, x_{i,j,2}, \ldots\ldots, x_{i,j,k}, \ldots\ldots, x_{i,j,n}\right\} \quad (2)$$

$$GRAD_{i,j} = max\left\{\left|x_{i,j,1} - \overline{x_{i,j}}\right|, \left|x_{i,j,2} - \overline{x_{i,j}}\right|, \ldots\ldots, \left|x_{i,j,k} - \overline{x_{i,j}}\right|, \ldots\ldots, \left|x_{i,j,n} - \overline{x_{i,j}}\right|\right\} \quad (3)$$

where $COV_{i,j}$, $MIN_{i,j}$, and $GRAD_{i,j}$ represent the coefficient of variation, the minimum and the gradient at the (*i,j*) position of the intensity image, respectively, and *k* is the ID of the images. False-colour images were composited with red, green and blue bands based on the results of these three features [40]. $COV_{i,j}$ and $GRAD_{i,j}$ represent the backscatter differences among the intensity images, and $MIN_{i,j}$ represents the minimum backscatter value for the same objects. A larger difference among the images and stronger backscattering correspond to brighter synthetic images. In addition, by introducing the TDX DEM, differential interferometric SAR (D-InSAR) process was applied to remove the terrain phase to generate coherence products of the PALSAR-1 data using the Gamma software developed by the Swiss company GAMMA Aktiengesellschaft (AG).

Six classes were extracted from the multi-temporal-intensity feature image and the coherence image. The labels for the different classes are listed in Figure 4. The six classes, i.e., red willow (class 1), reeds & splendid achnatherum (class 2), currently cultivated lands (class 3), water & wetland (class 4), sand dunes (class 5), and Gobi (class 6), were identified using the feature image and coherence image. The water, wetlands and sand dunes were extracted first, using coherence coefficient (CC) values lower than 0.25 for the initial classification; subsequently, this group was separated using the intensity feature images with a Maximum Likelihood Classifier (MLC). In this region, 90% of the currently cultivated lands are vineyards with a brighter colour, which indicates a strong backscatter and allows for easy identification. Different types of arid land vegetation (class 1 and class 2) can be distinguished with the *MIN* component of the intensity feature images, with class 1 plants exhibiting a larger and concentrated distribution of "brighter" backscattering power and class 2 plants exhibiting lower and dispersed "brighter" backscatter power. Both class 1 and class 2 are the target areas of potential ancient arable lands and the Daze range.

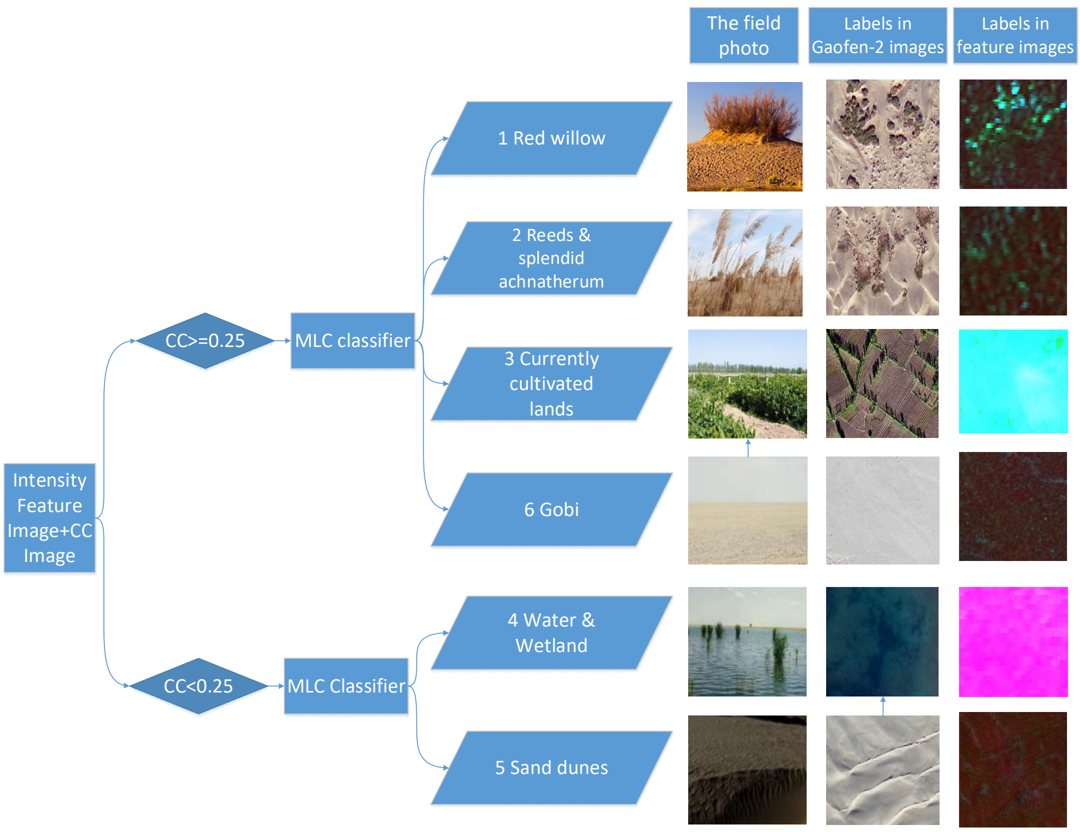

Figure 4. Classification approach and resulting classes based on the intensity feature image and the coherence coefficient (CC) information. A CC value of 0.25 is the threshold used to obtain the first classification, followed by the MLC to obtain the second classification and the final six classes including red willow (class 1), reeds & splendid achnatherum (class 2), currently cultivated lands (class 3), water & wetland (class 4), sand dunes (class 5) and Gobi (class 6). The field photos and the labels in the Gaofen-2 images and the intensity feature images for the different classes are shown.

2.3.3. Field Investigation and Reconstruction of the Han and Tang Dynasties Water Cultivation Paleoenvironment

The watershed, drainage network, and dried-up watercourses along with the ancient and current arable lands were overlaid on the 15-m Landsat 8, 0.8-m Gaofen-2 and KH images. Based on accessibility in the field, several sample points of the extracted target area of dried-up watercourses, the Daze range, and the potential abandoned arable area were investigated through an archaeological field survey. Together with historical documents of the Han and Tang dynasties, other target areas were validated using the deduction method based on similar characteristics. Subsequently, reconstruction was performed based on field verification and deduction.

3. Results and Fieldwork Verification

3.1. Ancient Water Distribution Based on the TDX DEM

3.1.1. Watershed Analysis and Drainage Network Extraction Based on the TDX DEM

The watershed and drainage network results are shown in Figure 5. For a larger area, including the Yumen frontier pass and Yangguan frontier pass, the results were extracted based on the 30-m SRTM DEM with an accumulation threshold of 1005, as shown in Figure 5a. For the Nanhu oasis, the same results were extracted using the 5-m TDX DEM with a threshold of 50,030, as shown in Figure 5b.

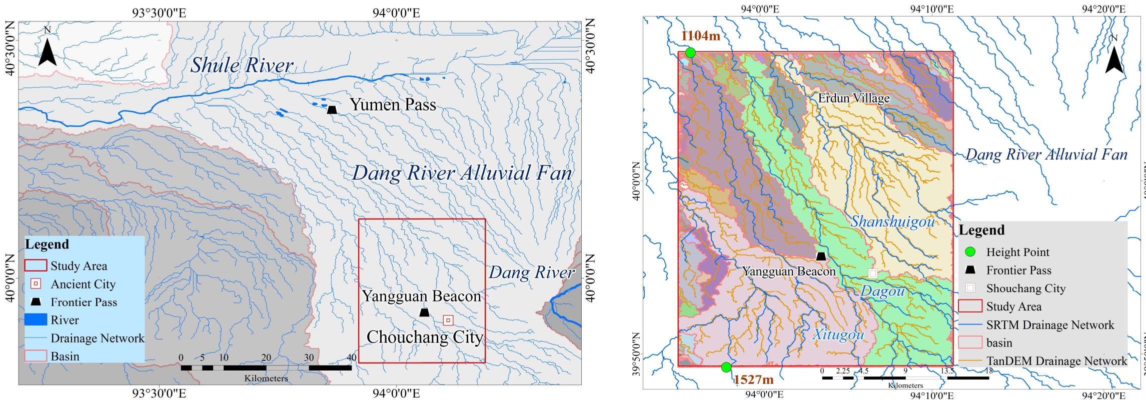

(a) (b)

Figure 5. (**a**) Watershed and drainage network extracted based on the 30-m SRTM DEM. (**b**) Watershed and drainage network extracted using the 5-m TDX DEM.

As shown in Figure 5a, the Shule River and the Dang River alluvial fan are located in the same basin as the Nanhu oasis, which indicates that all the streams of the alluvial fan entering the Shule River originate from the elevated southern areas and flow towards the depressed northern areas of the terrain. Because of the lower resolution of the SRTM DEM, the drainage network can be extracted from the TDX DEM data with higher accuracy and greater density. Based on the TDX DEM basin results, the Nanhu oasis decreases in elevation from south to north and extends about 16 km in length and 8 km in width at its widest. The highest altitude of 1527 m occurs at the southwest edge of the natural reserve and the lowest altitude of 1104 m is located in the northwest region. The relative height difference is approximately 423 m. Figure 5b also shows that the fine-resolution TDX DEM data are helpful for geomorphological catchment analyses and extractions of more detailed stream networks and watersheds. The results show that in the Nanhu oasis, the Wulujian (an ancient stream of the Tang Dynasty (618–907 A.D.), now the Xitugou), the Daqu (an ancient stream of the Han and Tang dynasties, now part of the Dagou) and the Shanshuigou (an ancient river with the same name as it has today) are located in three separate basins related to the three main cultivated zones.

3.1.2. Dried-Up Watercourse Extraction Based on the TDX DEM and Field Investigation

A comparison with the current drainage network shows that the results extracted from the TDX DEM not only identify the surface streams, including the Shanshuigou and Wulujian of the Tang Dynasty (618–907 A.D., now the Xitugou) but also ancient dried-up watercourses. The associated fieldwork was conducted to verify the target area in April 2018 with the Gansu Province Cultural Relic Institute of Archaeology and the Dunhuang Museum.

1 Westward dried-up watercourse of the Wulujian (now the Xitugou) of the Tang Dynasty

West Shouchang City was founded in 626 A.D. in the Tang Dynasty. The Wulujian extends due west into the city and was recorded to be 10 tangli (a distance unit used in the Tang Dynasty, with one tangli equivalent to 559.8 m) from the Yangguan woodlands [1]. Based on the drainage network extraction from the TDX DEM, a long dried-up east-west watercourse was connected to the current Xitugou. The extracted drainage network overlaid on the Gaofen-2 image and the shaded relief model are shown in Figure 6a,b, respectively. In Figure 6a, water is not present in the dried-up bed, and the watercourse is difficult to identify because of the lack of difference between the background and the watercourses covered by sand. Conversely, locating the watercourse is much easier using the drainage network extraction from the TDX DEM, as shown in Figure 6b. In the range of Figure 6b, the height differences between the thalweg and bank lines of the dried-up watercourses are between 8 and 11 m. This dried-up watercourse was verified by fieldwork to be the main source of irrigation for the ancient West Shouchang City, and the suspected city location was identified at the intersection of the east-west watercourse and the southeast-northwest watercourse. Today, the direction of the Xitugou is to the south, and West Shouchang City has been totally covered by sand.

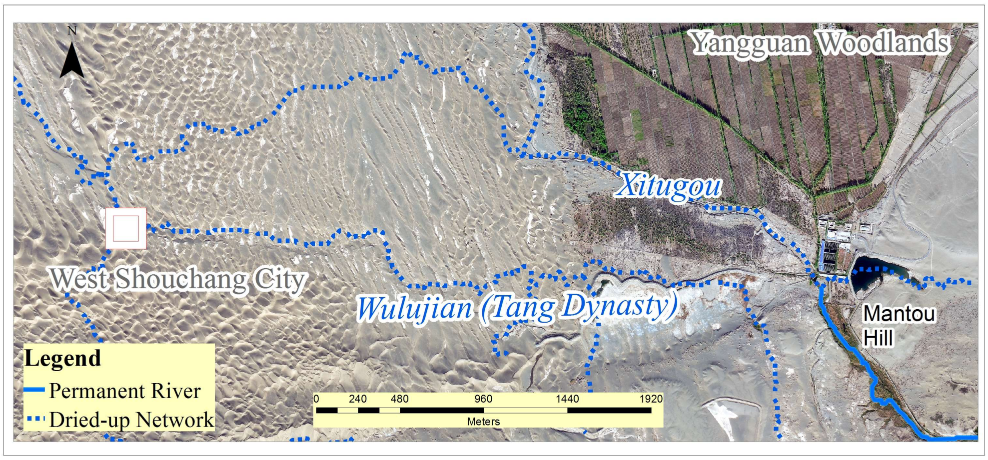

(**a**)

Figure 6. *Cont*.

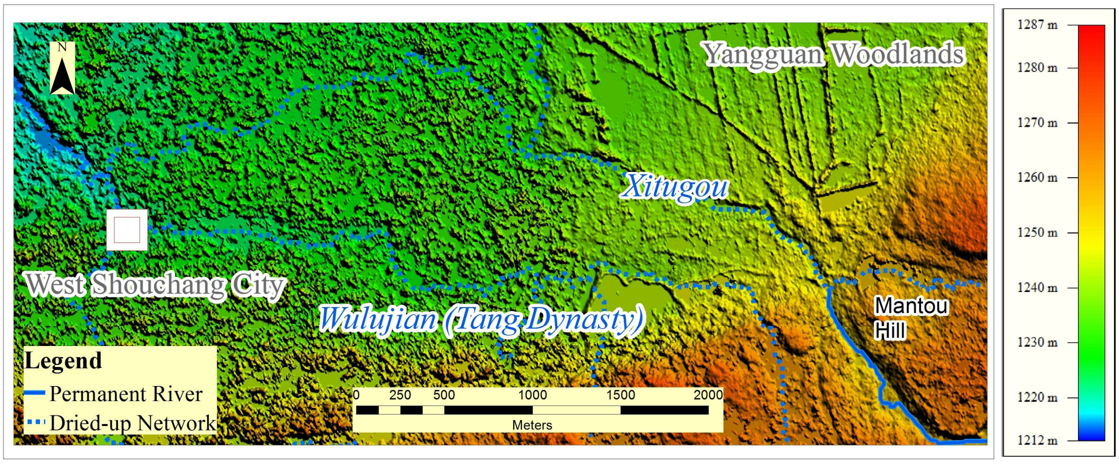

(**b**)

Figure 6. Dried-up watercourse of the Wulujian and the suspected location of West Shouchang City of the Tang Dynasty. (**a**) Extracted drainage network overlaid on the Gaofen-2 image; (**b**) extracted drainage network overlaid on the shaded relief model.

2 The dried-up watercourse of the source of the Shangbanao Spring and the location of the mysterious Daze range

Shangbanao Spring (headstream of the Dagou during the Han and Tang dynasties) [2] is located in East Gudongtan, and the northern part was buried by sand in the modern era. The drainage network extracted from the TDX DEM indicates that the spring water originated from the far southeast region. The river network results overlaid on the Gaofen-2 image and the TDX DEM are shown in Figure 7a,b, respectively. The field investigation showed traces of the river flow with red willows, as shown in Figure 7c,d.

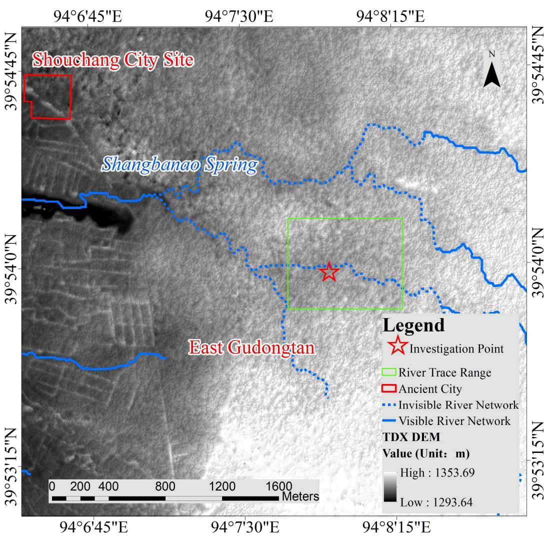

(**a**)

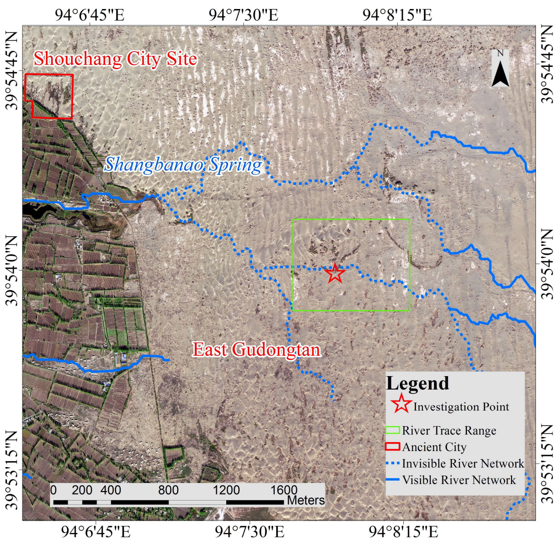

(**b**)

Figure 7. *Cont.*

(c) (d)

Figure 7. Extracted dried-up watercourse of the source of Shangbanao Spring and a field photo of the upstream area. (**a**) The extracted drainage network overlaid on the shaded relief model; (**b**) the extracted drainage network overlaid on the Gaofen-2 image; (**c**) traces of the river flow with red willows on the Gaofen-2 image; (**d**) field photo of red willows and reeds at the star location in (**c**).

Therefore, Shangbanao Spring is only the surface headstream of the Dagou, and the extracted dried-up watercourse shows that the groundwater sources trace far away to the southeast and are assumed to belong to the theorized northern border of the mysterious Daze range present during the Tang Dynasty (618–907 A.D.). Records indicate that the Daze range was 7 tangli (1918.6 m) south of Shouchang City and extended 10 tangli (5598 m) from east to west and 15 tangli (8397 m) from south to north. It was presumably located to the east of the Huangshuiba reservoir and south of the Shuangdunzi farmlands [1,14]. However, there is no indication on the VIR image of this ancient wetland range. The microrelief analysis of the TDX DEM data indicates that several dried-up watercourses, including the Honggou and Shagou, are supposedly located in the Daze range, as shown in Figure 8.

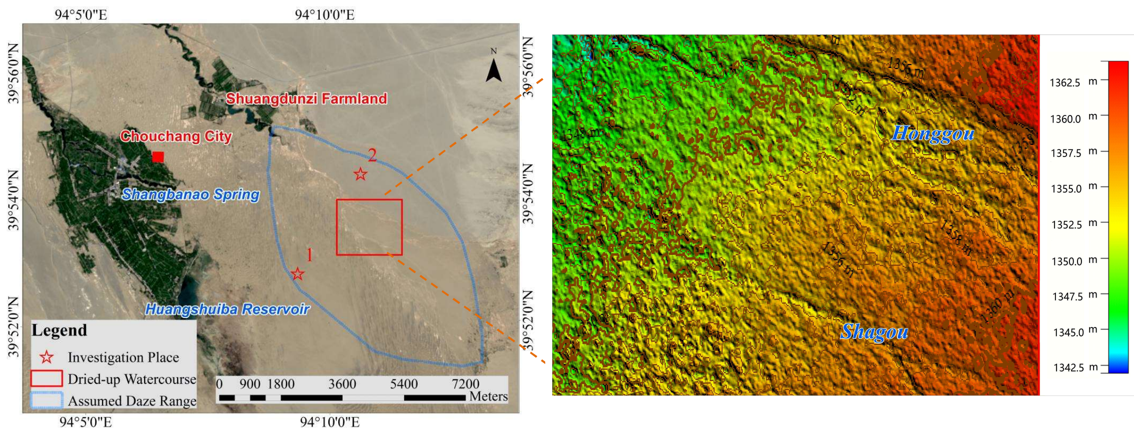

(a) (b)

Figure 8. Upstream dried-up watercourses of the Shagou and Honggou located in the assumed range of the Daze during the Tang Dynasty. (**a**) Location of the dried-up watercourses on the Landsat 8 OLI image; (**b**) shaded relief model of the dried-up watercourses Shagou and Honggou.

Two sample locations were investigated during the fieldwork. One is located in Gobi in an area with few or no arid land vegetation, and the other is located in the Yangguan National Natural Reserve, where arid land vegetation is present, as shown in Figure 8a. Interestingly, at both sample locations, the soil profiles exhibit cross-sectional layers shaped like the letter "V" approximately 20 cm below the surface, as shown in Figure 9a,b; these features are assumed to be spring vents. This finding indicates that many springs were distributed in the range of the largest ancient wetland in the Nanhu region [1].

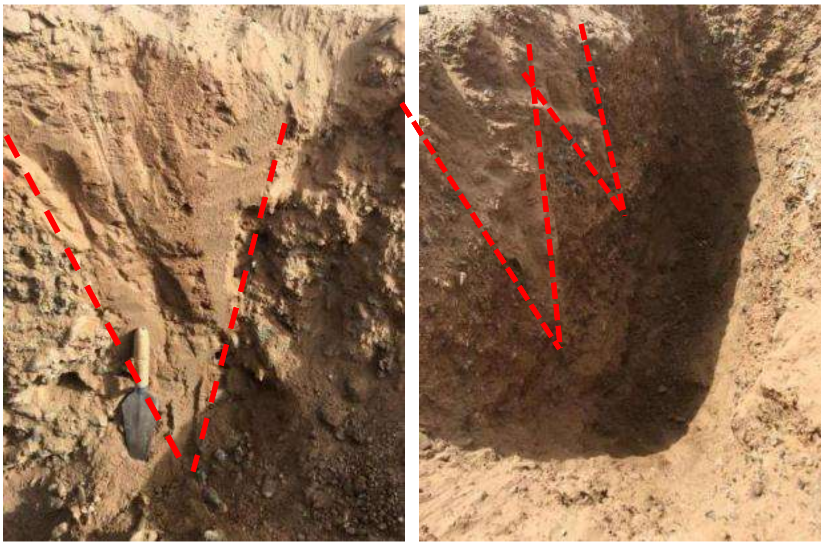

(**a**) (**b**)

Figure 9. Soil profiles of two sample locations in the alluvial fan; both locations exhibit cross-sectional features shaped like the letter "V" approximately 20 cm below the surface with clear sand and gravel layers. (**a**) Field photo of sample location 1 in the Gobi near the Shuangdunzi; (**b**) field photo of sample location 2 near the Huangshuiba Reservoir.

The field investigation also identified a destroyed dam and an abandoned road constructed in the 1970s (shown in Figure 10a, b), demonstrating that surface water sources were still flooding this area in the 1970s, and that the area presumably represented the upstream area of the Daze range.

(**a**) (**b**)

Figure 10. Destroyed dam on the Honggou and a 10-m-wide abandoned road found during the field investigation. (**a**) Field photo of the destroyed dam across the dried-up watercourses; (**b**) field photo of the abandoned road discovered near the dried-up watercourses.

3.2. Cultivated Land Extraction with PALSAR-1

3.2.1. Information Extraction with PALSAR-1

The false colour image composited by the *COV*, *MIN* and *GRAD* values based on six scenes of the time-series PALSAR-1 images is shown in Figure 11a. The D-InSAR technique was applied to all the combinations of the two scenes and the interferogram of the two scenes acquired on 6 October 2010 and 21 February 2011, with the best coherence being shown in Figure 11b. The tree classification result is shown in Figure 11c; it shows 5 classes, including currently cultivated land, desert and Gobi, water and wetland, red willow, and reed and splendid achnatherum. Some classification errors caused by electric poles or terrain influences are observed but can be eliminated by visual interpretation.

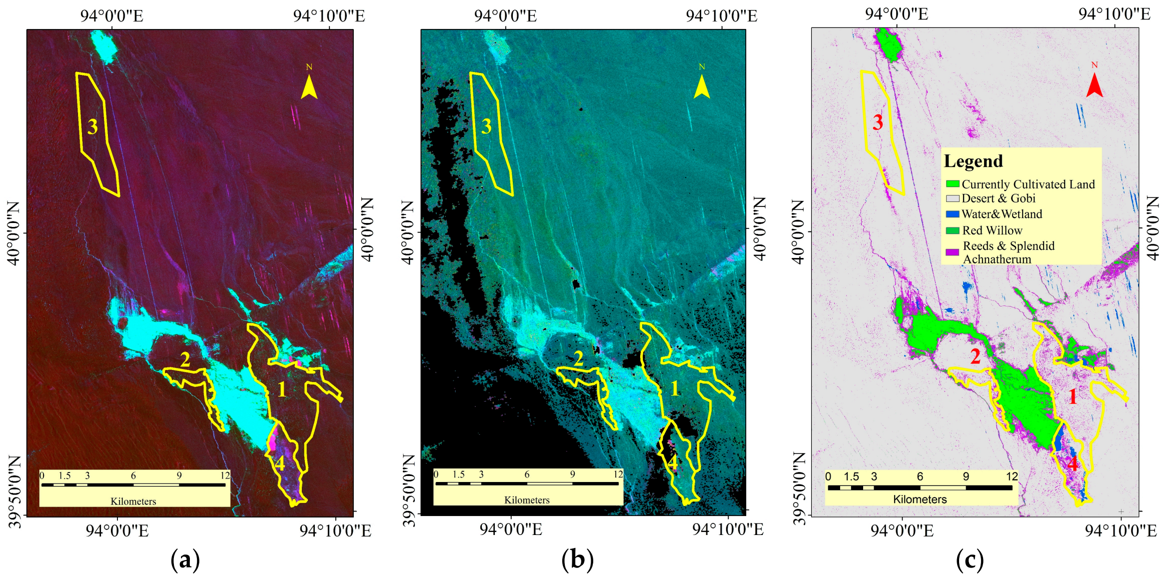

Figure 11. Feature extraction using multi-temporal PALSAR-1 images. (**a**) Intensity feature composite images; (**b**) D-InSAR interferogram with a CC value greater than 0.25; (**c**) classification results.

In Figure 11a, most of the "red" areas consist of sand dunes, which change over time and have a higher variation coefficient but lower backscattering and gradient values. The brighter "blue" or "green" areas indicate rural areas or surface streams (Shanshuigou and Xitugou), which exhibit higher backscattering. The bright "purple" areas are surface water or streams with seasonal variation that display higher coefficient of variation and gradient values, along with lower backscatter, due to their specular reflection. Four target areas of "anomalies" are labelled in Figure 11a. The regions of arid land vegetation (1, 2, and 3) exhibit "bright or dark green" speckles. In Figure 11b, an obvious decorrelation is observed for the water and sand dunes located in the southwestern area. Higher backscattering power is observed for the cultivated areas and lower backscattering power is observed for the Gobi, water and desert areas.

3.2.2. Arid Land Vegetation Analysis and Estimation of the Potential Ancient Arable Range

PALSAR-1 was applied to extract the arid land vegetation that serves as an indicator of potential ancient arable land. The associated fieldwork was conducted in November 2017 with the Gansu Province Cultural Relic Institute of Archaeology and the Dunhuang Museum. During the field investigation, more channels were found in the reeds and splendid achnatherum target area than in the red willow area. That is, arid land vegetation is a positive sign of the archaeological targets and the depth to the groundwater has to be considered. Because the state and distribution of psammophytes, such as red willow, and phreatophytes, such as reeds, change as the groundwater level changes, shown in Figure 12.

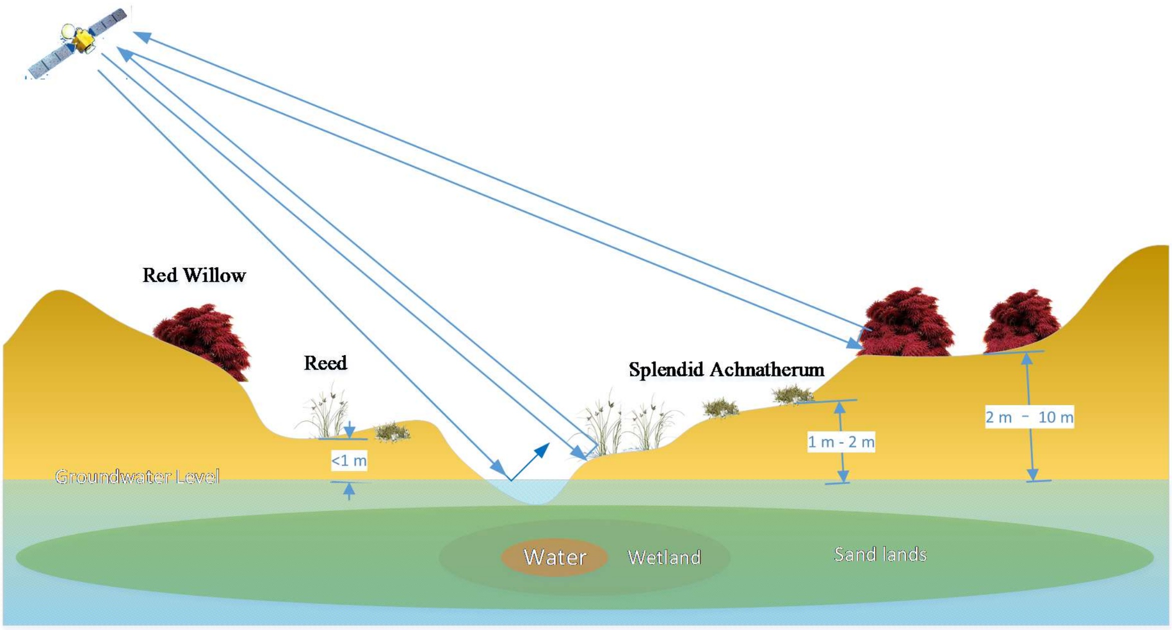

Figure 12. The correlation between arid land vegetation and the groundwater level. As a depth to the groundwater of less than 2 m, phreatophytes including reeds and splendid achnatherum are the dominant plants; at a depth between 2 m and 10 m, psammophytes are the dominant plants; at a depth greater than 10 m, few plants are found [41].

In terms of archaeological discovery, targets such as ditches and channels are easier to detect if they are covered by less sand. Therefore, in this study, reeds and splendid achnatherum provide better information than red willow for detecting potential ancient arable lands. The classification result shown in Figure 11c indicates that the reeds and splendid achnatherum are distributed near the currently cultivated land, especially in Gudongtan (Area 2), East Gudongtan (Area 1), and the downstream area of the Xitugou (Area 3), where potential ancient arable lands may have been located.

In target area 2, located in Gudongtan, many records indicate that farmlands and cultivated areas were distributed throughout the region, with abandoned channels, pottery tiles and ridges indicating the presence of plentiful groundwater in the Han and Tang dynasties [1].

Target area 1 is located in East Gudongtan upstream of Shangbanao Spring. The plant distribution shows that this area is connected to Shanshuigou, and the water source is located to the southeast, which is consistent with the TDX DEM results. This area of rich groundwater is presumed to be the ancient northern border of the Daze range in the Tang Dynasty (618–907 A.D.). During the fieldwork, several abandoned channels were found at the west edge of East Gudongtan, as shown in Figure 13. The desertification of East Gudongtan is becoming increasingly serious; the abandoned channels presumably brought water for irrigation from the Wowashui to East Gudongtan and the ancient Shouchang City of the Tang Dynasty (618–907 A.D.). The submeter high-resolution Gaofen-2 image is useful for identifying additional 1-m abandoned channels or ridges that exhibit the same texture and appear on the images as linear tracks or linear distributions of vegetation. During the field investigation, we observed these linear channel tracks filled with reeds. We used the historical material for a preliminary identifiction of the abandoned channels, such as the Changzhi channel and its associated small channels, which were located approximately 500 m away from the edge of the currently cultivated land. This finding demonstrates that target area 1 was likely part of the cultivated area during the Tang Dynasty (618–907 A.D.).

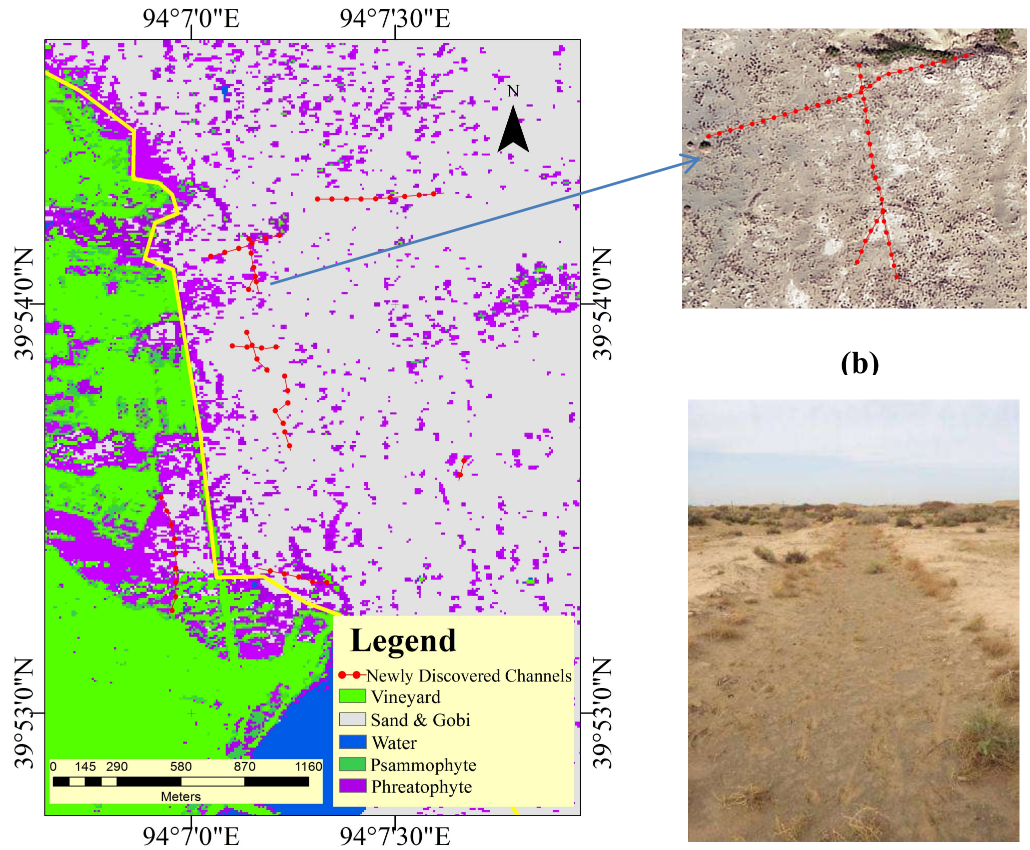

(a) (c)

Figure 13. Images and field photos of abandoned channels located in area 1 of East Gudongtan. (**a**) The abandoned channels on the classified images; (**b**) the channels on the Gaofen-2 image; (**c**) photo of one of the abandoned channels.

Target area 3 is located downstream of the Wulujian present in the Tang Dynasty (618–907 A.D., now the Xitugou). Through field investigation, many linear features, ridge traces, and regular shapes of artificial objects were observed in area 3, approximately 11 kilometres away from the Nanhu woodlands and southeast of the No. D87 beacon tower, as shown in Figure 14a. The channels were distributed in a large area with an extent of 1.8 km east-west and 7 km north-south. The regularly shaped object was the newly discovered remnants of a farmhouse with pottery and porcelain tiles from the Ming and Qing dynasties; this building was hypothesized to have been located downstream of the cultivated area and was abandoned at least since the reign of these dynasties. Around the newly discovered arable area, a new beacon tower was discovered in the west, as shown in Figure 14a. This beacon tower is helpful for locating the assumed Great Wall trenches between D87 and the Yanjiamiao Beacon Tower. The trenches passed along the western side of the arable area and indicate that the arable area has been cultivated since the Han and Tang dynasties. This finding is also useful for locating the Yangguan frontier pass, which is assumed to be located at the point where the Silk Road intersects the north-south-oriented Great Wall.

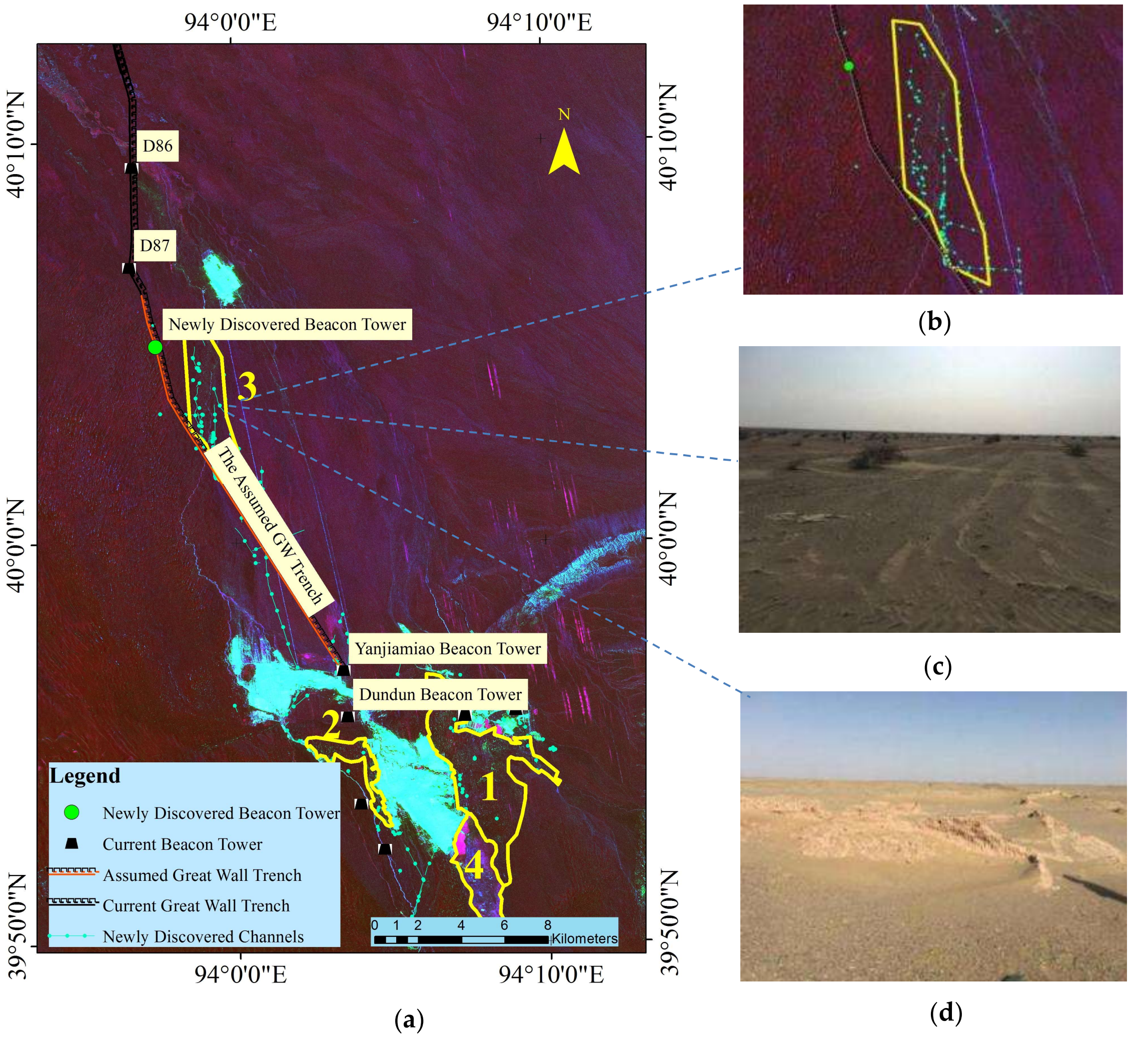

Figure 14. (**a**) The location of target 3 with the assumed Great Wall trench and beacon towers overlaid on the composite results; (**b**) the location of target 3 and the abandoned channels, ridges, and a newly discovered beacon tower; (**c**) field photos of the abandoned channels and ridges; (**d**) a farmhouse located in area 3.

3.3. Reconstruction of the Water Cultivation Paleoenvironment Dating Back to the Han and Tang Dynasties

Based on the extraction results verified by fieldwork using spaceborne SAR and archaeological documents, the water cultivation paleoenvironment was reconstructed dating back to the Han and Tang dynasties. The results are shown in Figure 15a; all place names are labelled with those used in the Tang Dynasty (618–907 A.D., an index with the names of the rivers, mountains and locations is provided in Appendix A).

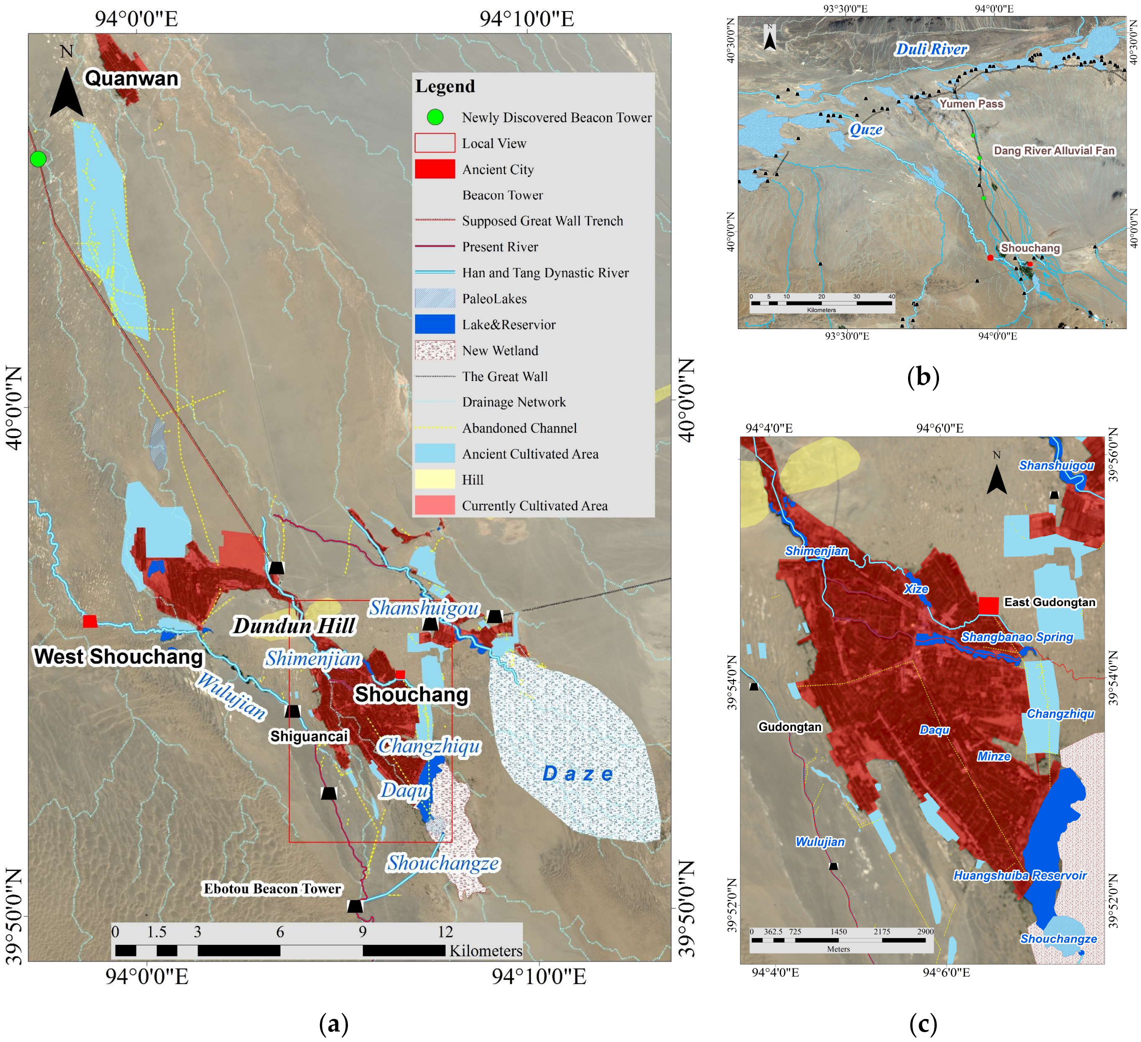

Figure 15. (**a**) Reconstruction of the water cultivation paleoenvironment of the Han and Tang dynasties; (**b**) water cultivation distribution of the Nanhu oasis in the Yangguan-Yumen frontier pass area; (**c**) magnified view of the area outlined in red in (**a**).

4. Discussion

4.1. Evolution of the Water Environment

Longle County (Shouchang during the Tang Dynasty) and the Yangguan frontier pass were initially established in the Nanhu oasis during the Western Han Dynasty (202 B.C.–8 A.D.). The waterways included the Wowashui (Shouchangze of the Tang Dynasty), Wulujian, Shimenjian and two channels, the Daqu and Changzhiqu [1]. The Wulujian originated from the spring close to the Shiguancai and the current water source of Ebotou Spring was historically connected with the Wowashui. After the Sui Dynasty (581–618 A.D.), severe desertification occurred in Gudongtan and the Yangguan frontier pass was abandoned. Longle County was renamed ancient Shouchang City. North of Shouchang City, five wetlands were present: Shouchangze (known as Wowashui during the Han Dynasty), Minze, Daze, Shangbanao, and Longquandui. Three streams, i.e., the Wulujian, Shimenjian, and Shanshuigou, were the main surface streams, as shown in Figure 15a. The Wulujian flowed west (Figure 6a) and irrigated West Shouchang City and reached Quze (the Yushu Spring basin downstream of the Shule River) and the Duli River (the Jiduanshui during the Han Dynasty (202 B.C.–220 A.D.), now the Shule River), as shown in Figure 15b. The Shanshuigou first originated in the Late Tang Dynasty (618–907 A.D.) as shown in Figure 15a. After the Yuan and Ming dynasties, the western part of the Wulujian was blocked, and its watercourse changed to the northeast towards the Quanwan, and West Shouchang City subsequently declined. Today, the Xitugou, which is the ancient Wulujian, is sourced from Ebotou Spring. Most of the five wetlands and channels have disappeared. Shouchang City, which is located in East Gudongtan, was partly covered by sand. The watercourses of the Xitugou and Shanshuigou deepened, and a new wetland other than the Daze formed when the Huangshuiba reservoir was constructed in the 1960s; this was also evidenced by a soil moisture anomaly and the reed cover extracted from the PALSAR-1 images in Figure 16a. Spring water leakage represents the main source of the new wetland, which covers the Wowashui.

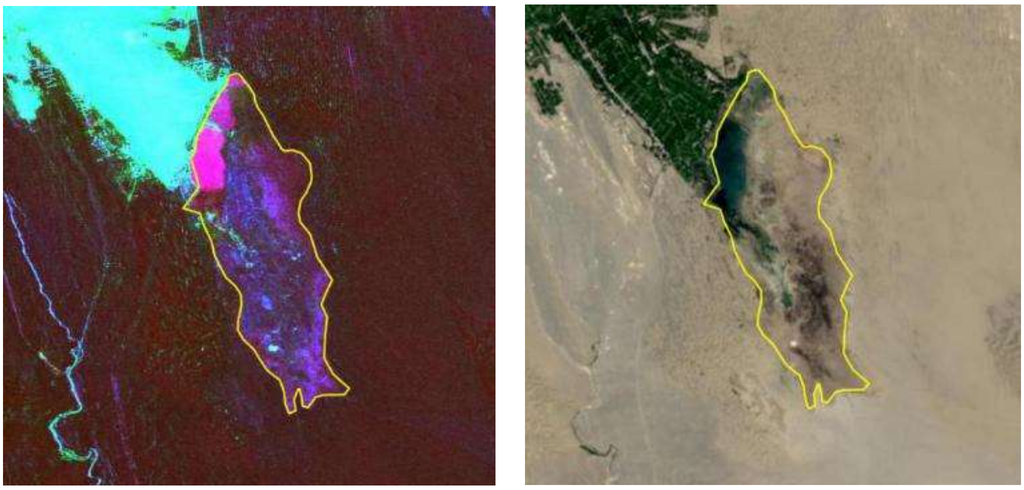

(**a**) (**b**)

Figure 16. (**a**) New wetland area extracted using PALSAR-1 data. (**b**) New wetland area overlaid on the Landsat 8 OLI image.

4.2. Evolution of the Cultivated Areas

The garrison and the army town at the Yangguan frontier pass was established in the Western Han Dynasty (202 B.C.–8 A.D.) [42]. The main water sources were the Wulujian and Wowashui. The cultivated area included Longle County and the Gudongtan, where large amounts of pottery and farmland ridges associated with the Han Dynasty (202 B.C.–220 A.D.) were found in area 3, which is shown in Figure 11a. The cultivated areas were further expanded and reached a peak in the Late Tang Dynasty (618–907 A.D.). The two main channels, the Shanshuigou and Daze, and West Shouchang City provided proof of the further increase in the cultivated area. In addition to cultivation during the Han Dynasty (202 B.C.–220 A.D.), the following areas were observed and verified:

- Farmland in East Gudongtan. Through field investigation and extraction of the target area with the SAR data, it was determined that the water sources of this area originated from the Daze and Changzhiqu, which delivered water from the Wowashui. Pottery tiles and discarded channels with reeds were found approximately 500 m away from the Nanhu oasis, supporting the hypothesis that the ancient cultivated areas date back to at least the Tang Dynasty.
- The downstream areas of Wulujian (Xitugou). Through PALSAR-1 target extraction and field verification, a beacon tower, several discarded channels, farming ridges, and a farmhouse were identified in this area, supporting Stein's conclusions that irrigated farmland was likely located approximately 300 km downstream of the area north of Dundun Hill [43]. All the results support that prior to the Ming Dynasty, even the Han and Tang dynasties, the water levels could have met the irrigation needs of this site.

4.3. Comparison of Current and Ancient Cultivated Areas

With the water sources of the Daze, the Wowashui, and two channels, the cultivated area in the range of the modern oasis may have also been irrigated during the Han and Tang dynasties. A comparison with the arable land results extracted from the TSX/TDX data showed that the large arable areas, including Eastern Gudongtan, Gudongtan, and the downstream area, were abandoned in the modern era. Most of the abandoned areas have been covered by sand, especially Eastern Gudongtan, where significant wind erosion of bare lands and the formation of large dunes have occurred since the 1910s as recorded by Stein and shown in Figure 17a.

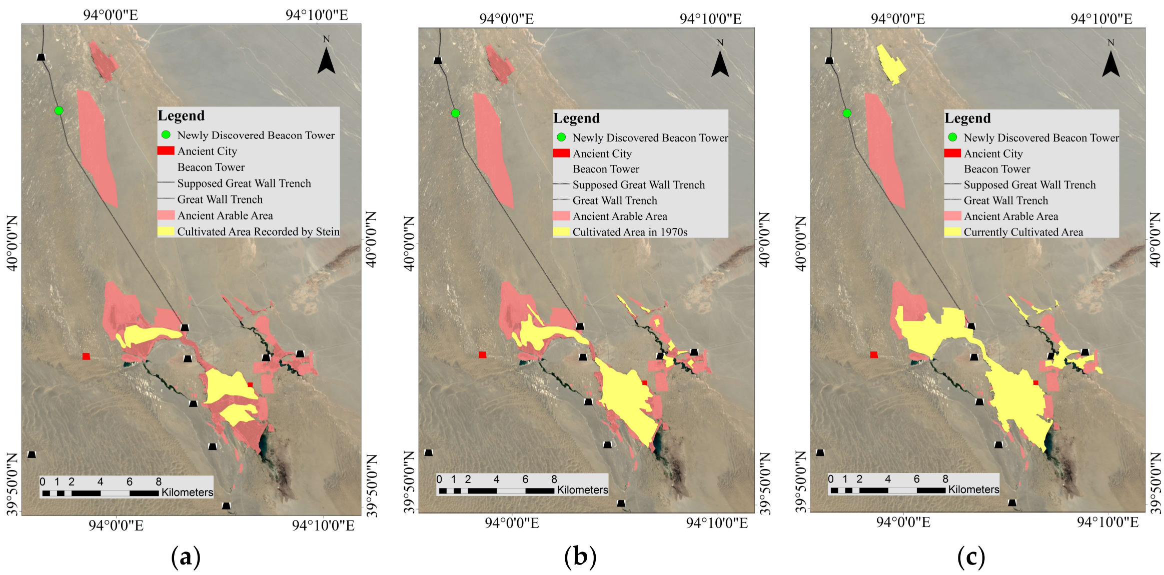

Figure 17. (**a**) Cultivated areas recorded by Stein in the 1910s; (**b**) cultivated areas in the 1970s extracted from Key Hole (KH) satellite images; (**c**) currently cultivated areas extracted from PALSAR-1 data.

Figure 17 shows that the cultivated area increased from the 1910s to the 1970s and to the present time. According to the extracted results verified by the field survey, the largest area of verified ancient arable land is 47.86 km^2, as shown in Figure 15, which is nearly two-times larger than that of the current range of arable land (25.78 km^2) shown in Figure 17c. However, there is contradictory evidence regarding the farming area and the population records. Based on the recorded population in the Book of Han, the area contained more than 11,200 households, including 38,335 people in Dunhuang County. Shouchang City had 359 households and a population of 1809 people. In 1991, a total of 1135 households with 4506 people were recorded in the town of Nanhu, which is three times higher than that in the Late Tang Dynasty (618–907 A.D.). A decrease in the population due to the use of traditional farming tools for these large cultivated areas seems unlikely, and the only reasonable explanation is that the population record was not updated after the Han Dynasty (202 B.C.–220 A.D.) and a population increase occurred during the Late Tang Dynasty [1].

4.4. Protection of the Water Cultivation Environment of the Nanhu Oasis

The garrison guaranteed long-term troop defence of the Silk Road trade during the Han and Tang dynasties (202 B.C.–907 A.D.). A large-scale channel system was established to develop military farming and exploit the wildlands. From the Han Dynasty (202 B.C.–220 A.D.) onward, the area occupied by the garrison in the Dunhuang region benefited from the rich water source of the Dizhishui (called the Ganquanshui during the Tang Dynasty (618–907 A.D.), now the Dang River) and flourished as a result [44,45]. However, large-scale cultivation led to a final drought and cutoff of the Nanjiduanshui River during the Han Dynasty (the Duli River of the Tang Dynasty, now the Shule River), representing one of the reasons for the desertification of the Nanhu oasis [46–50]. Precipitation and spring runoff were the basic water sources for the ancient Nanhu oasis. Climatically, the Yangguan frontier pass town is located in a warm temperate arid area and the water source is the Altan water conservation area, which receives concentrated precipitation from June to September. Records indicate that strong changes in precipitation and climate did not occur from the Han and the Western Liang dynasties, and the precipitation varied by 8.0% over this period. After 400 A.D., the precipitation increased, and the rainfall was sufficient for agriculture, thus accounting for the large increase in arable area. Currently, the main water source of the Nanhu basin is underground seepage of the Dang River, whose sources are the melting of ice and snow in the Qilian and Altyn mountains. Due to the acceleration of glacial recession and decreasing groundwater discharge, wetland areas have experienced considerable shrinkage and vegetation degradation [12]. During the 1960s to the 1970s, newly built dams cut off the upstream flow of the Dang River, which further aggravated these trends. The riverbeds became covered by sand, land desertification intensified, and several abandoned farmlands were covered by sand dunes with heights of 3–5 m and intervals of 40–60 m. These findings explain why the current arable land area is much smaller than in the Han and Tang dynasties. In recent decades, as the population has continued to increase, the area of cultivated land has gradually expanded due to deforestation. Crops with high water demands, such as the cotton were planted in Dunhuang, causing a surge in agricultural irrigation and resulting in the exploitation of a large amount of groundwater. This, in turn, resulted in a continuous decline in the groundwater level since the 1990s [51] and drought and degradation of cultivated areas in the downstream regions. Therefore, the protection of the water cultivation environment and appropriate use of oasis water and wetland sources have crucial significance for the protection of the Nanhu oasis and Yangguan frontier pass as heritage sites [52].

5. Conclusions

As a result of sufficient groundwater, the garrison reclamation of the Nanhu oasis, the westernmost oasis of the Hexi Corridor, guaranteed long-term southern route frontier defence and trade on the Silk Road from the Han to the Tang dynasties. Due to the deterioration of the local environment and increased activity on the maritime Silk Road, the Yangguan frontier pass was finally abandoned, resulting in most of the arable garrison areas being covered by sand. The reconstruction of the water cultivation paleoenvironment provides an in-depth understanding of the garrison-defended ecosystem and facilitates the recovery of historical remains. Because of environmental deterioration and site inaccessibility, spaceborne remote sensing technology is helpful for pinpointing target area for archaeological surveys. The selection of suitable data sources to investigate a target and an appropriate remote sensing extraction model improve the cost-effectiveness of archaeological surveys. The following conclusions are drawn.

1. The proposed workflow of archaeological water cultivation information extraction with the X-band and L-band spaceborne SAR data was successfully applied to the Nanhu oasis. A 5-m DEM was generated from the X-band TSX/TDX data and used for the microrelief analyses. Using a watershed analysis and drainage network extraction, the dried-up watercourses were detected and precisely described and the upstream area of the Daze range was located. Furthermore, by exploiting the correlation between the groundwater level and the arid land vegetation, especially the reeds and splendid achnatherum, and the hydrological sensitivity of the multi-temporal L-band SAR, we estimated the potential ancient arable target area for the archaeological survey using both the backscattering and coherence characteristics of PALSAR-1 data.
2. An archaeological investigation of the target area was conducted to verify the results of the method, which led to the discovery of a beacon tower, several dried-up paleochannels and ditches, and farmland. The dried-up paleochannels included the westward ancient dried-up watercourse of the Wulujian, the source of Shangbanao Spring, and the upstream area of the Daze range (a wetland area during the Tang Dynasty (618–907 A.D.)). Large-scale ditches were

found in East Gudongtan and the downstream area of the Xitugou. These findings are helpful for further archaeological interpretation and archaeological validation.

3. Subsequently, a reconstruction map of the water cultivation paleoenvironment of the Nanhu oasis was generated. Combined with historical material, the evolution of the watercourses and cultivated areas dating back to the Han and Tang dynasties was discussed. From the Han to Tang dynasties, the verified arable area in the Nanhu oasis was nearly twice that of the current area. The analysis of the degradation of the irrigated areas indicates that the restriction of the use of groundwater and wetland conservation is important for the protection of the water cultivation environment of the Nanhu oasis.

Author Contributions: X.Z., F.C. and H.G. conceived and designed the experiments; X.Z. and F.C. performed the experiments and field investigation and analysed the data; H.G. provided advice regarding the methods and their application; and X.Z. wrote the paper.

Funding: This research was funded by the Strategic Priority Research Program of the Chinese Academy of Sciences (Grant No. XDA19030502), the National Natural Science Foundation of China (NSFC) (Grant No. 41771489), the CAS-TWAS Centre of Excellence on Space Technology for Disaster Mitigation "Joint Program on Space Technology for Disaster Mitigation for Belt and Road Initiative", and the Hundred Talents Program of the Chinese Academy of Sciences (Grant No. Y5YR0300QM), Academic Leader Funding Key Laboratory of Earth Observation and Geospatial Information Science of NASG.

Acknowledgments: We acknowledge support of the Gansu Province Cultural Relic Institute of Archaeology, and the Dunhuang Museum..

Conflicts of Interest: The authors declare no conflicts of interest.

Appendix A

Table A1. Index of the names of the rivers, mountains and locations used in the paper

Types	Name in the Han Dynasty (202 B.C.–220 A.D.)	Name in the Tang Dynasty (618–907 A.D.)	Current Name
River	Dizhishui	Ganquanshui	Dang River
River	Nanjiduanshui	Dulihe	Shule River
Wetland	-	Quze	Yushu Spring Base
Lake	Wowashui	Shouchangze	Near Daquan Spring
Lake	Puchanghai	Puchanghai	Luoupo
Wetland	-	Daze	-
Wetland	-	Longquandui	-
Channel	Daqu	Daqu	Part of Dagou
Channel	Changzhiqu	Changzhiqu	-
Stream	-	Shanshuigou	Shanshuigou
Stream	Shimenjian	Shimenjian	-
Stream	Wulujian	Wulujian	Xitugou
Place Name	Ebotou Spring	Ebotou Spring	Ebotou Spring
Place Name	Shangbanao	Shangbanao	Shangbanao
Place Name	Longle County	Choushang City	Pochengzi
Place Name	Dunhuang Jun	Shazhou City	Dunhuang
Place Name	-	West Shouchang City	-
Mountain	Longmen	Shimen	Dundun
Mountain	Longle	Longle	Altun
Mountain	-	Shashan	Shashan

References

1. Li, Z. *The Ancient Dunhuang Local Chronicles Eight Commentary*; Gansu People's Publishing House: Gansu, China, 2007; ISBN 9787226035603.
2. Stein, M.A. *From Luobo Desert to Dunhuang*; Guangxi Normal University Press: Guangxi, China, 2000; ISBN 7-5633-3078-X.
3. Wu, C.; Xie, J.; Zhao, T.; Liu, X. Study on the best band of TM remote sensing image- illustrated by the case of Yangguan National Nature Reserve of Dunhuang, Gansu. *Gansu Sci. Technol.* **2016**, *32*, 21–24. [CrossRef]
4. Guo, Q.; Wang, X.; Li, Z.; Zhang, L. Condition survey and conservation of Dunhuang Yangguan pass beacon. *Dunhuang Res.* **2007**. [CrossRef]
5. Li, Z. *Conservation of Ancient Sites on the Silk Road*; Science Press: Beijing, China, 2003; ISBN 9787030107145.
6. He, W.; Dai, X. Study on wetland reserve sustainable utilization and main problems of Yangguan in Dunhuang. *Gansu Sci. Technol.* **2014**, *30*. [CrossRef]
7. Chen, M. Current status of wetland environment in Dunhuang and countermeasures for protection and restoration. *Wetl. Sci. Manag.* **2007**, *3*, 38–41. [CrossRef]
8. Xie, F. Distribution Characteristics of Plant Diversity of West Lake Nature Reserve in Dunhuang and Its Response to Soil Factors. Master's Thesis, Lanzhou University of Technology, Gansu, China, 2014.
9. Dai, X.; Dong, Z.; Xie, J. Analysis on the biological diversity and protective strategy in nature reserve of Yangguan in Dunhuang China. *Chin. J. Popul. Resour. Environ.* **2014**, *24*, 389–392.
10. Dai, X.; Xie, J.; Wang, M.; Dong, Z. Chracteristics of plant communities and species diversity in wetlands in Yangguan national nature reserve in Dunhuang. *Wetl. Sci.* **2015**, *13*, 381–385. [CrossRef]
11. Sun, S. Study on the land use change in Dunhuang Xihu based on Landsat images. Master's Thesis, China University of Geosciences, Beijing, China, 2017.
12. Duan, H.; Pan, S.; Li, L.; Yuan, H. Analysis on wetland evolution and its driving factors of Dunhuang Xihu nature protection area. *Geo-Inf. Sci.* **2015**, *17*, 222–228.
13. Wu, C. Study on Application of 3S technology in the national natural reserve of Yangguan in Dunhuang. *Gansu Sci. Technol.* **2013**, *29*, 49–52. [CrossRef]
14. Wu, R. *Investigation and Study of Hexi passes of Han Dynasty*; Cultural Relics Publishing House: Beijing, China, 2005.
15. Liu, Y. The Study on the Relationship between Water Environmental Characteristics and Cultural Relics in Yangguan Town, Dunhuang City. Master's Thesis, Gansu University, Gansu, China, 2015.
16. Ji, Z.; Ji, Y. *Essays of Yumen and Yangguan in Dunhuang*; Gansu People's Publishing House: Gansu, China, 2003.
17. Tapete, D.; Cigna, F. Trends and perspectives of space-borne SAR remote sensing for archaeological landscape and cultural heritage applications. *J. Archaeol. Sci. Rep.* **2016**, *14*, 716–726. [CrossRef]
18. Tapete, D.; Cigna, F.; Donoghue, D.N.M. 'Looting marks' in space-borne SAR imagery measuring rates of archaeological looting in Apamea (Syria) with TerraSAR-X staring spotlight. *Remote Sens. Environ.* **2016**, *178*, 42–58. [CrossRef]
19. Chen, F.; Lasaponara, R.; Masini, N. An overview of satellite synthetic aperture radar remote sensing in archaeology: From site detection to monitoring. *J. Cult. Heritage* **2017**, 5–11. [CrossRef]
20. Lasaponara, R.; Masini, N. Satellite Synthetic Aperture Radar in archaeology and cultural landscape: An overview. *Archaeol. Prospect.* **2013**, *20*, 71–78. [CrossRef]
21. Chen, F.; Masini, N.; Liu, J.; Lasaponara, R. Multi-frequency satellite radar imaging of cultural heritage: The case studies of the Yumen Frontier Pass and Niya ruins in the western regions of the Silk Road corridor. *Int. J. Digit. Earth* **2016**, *9*, 1224–1241. [CrossRef]
22. McCauley, J.F.; Schaber, G.G.; Breed, C.S.; Grolier, M.J.; Haynes, C.V.; Issawi, B.; Elachi, C.; Blom, R. Subsurface valleys and geoarchaeology of the Eastern Sahara revealed by Shuttle SAR. *Science* **1982**, *218*, 1004–1020. [CrossRef] [PubMed]
23. Lu, X.; Guo, H.; Shao, Y. Detection of the Great Wall using SIR-C data in north-western China. In Proceedings of the International Geoscience and Remote Sensing Symposium (IGARSS), Singapore, 3–8 August 1997.
24. Erasmi, S.; Rosenbauer, R.; Buchbach, R.; Busche, T.; Rutishauser, S. Evaluating the quality and accuracy of TanDEM-X digital elevation models at archaeological sites in the cilician plain, Turkey. *Remote Sens.* **2014**, *6*, 9475–9493. [CrossRef]

25. Tang, P.; Chen, F.; Zhu, X.; Zhou, W. Monitoring cultural heritage sites with advanced multi-temporal InSAR technique: The case study of the summer palace. *Remote Sens.* **2016**, *8*, 432–446. [CrossRef]
26. Paillou, P.; Lopez, S.; Farr, T.; Rosenqvist, A. Mapping subsurface geology in Sahara using L-Band SAR: First results from the ALOS/PALSAR. *IEEE J. Sel. Top. Appl. Earth Obs. Remote Sens.* **2010**, *3*, 632–636. [CrossRef]
27. Paillou, P.; Lopez, S.; Lasne, Y.; Rosenqvist, A.; Farr, T. Mapping subsurface geology in arid Africa using L-band SAR. In Proceedings of the 2007 IEEE International Geoscience and Remote Sensing Symposium, Barcelona, Spain, 23–28 July 2007; pp. 2685–2688.
28. Du, Q.; Chai, L.; Fan, S.; Ma, P. The geological resources survey and geoscience significance of Dunhuang Yardang National Geopark in China. *J. Desert Res.* **2016**, *36*, 610–615. [CrossRef]
29. China's Surface International Exchange Station's Daily Climate Dataset. Available online: http://data.cma.cn/data/detail/dataCode/SURF_CLI_CHN_MUL_DAY_CES_V3.0.html (accessed on 16 May 2018).
30. Introduction of TDX (TanDEM-X: TerraSAR-X Add-on for Digital Elevation Measurement). Available online: https://directory.eoportal.org/web/eoportal/satellite-missions/t/tandem-x (accessed on 16 May 2018).
31. Du, Y.; Feng, G.; Li, Z.; Zhu, J.; Peng, X. Generation of high precision DEM from TeraSAR-X/TanDEM-X. *Chin. J. Geophys.* **2015**, *58*, 3090–3102. [CrossRef]
32. Gaofen-2 Data. Available online: https://www.satimagingcorp.com/satellite-sensors/gaofen-2/ (accessed on 16 August 2018).
33. Landsat 8 Data. Available online: https://landsat.usgs.gov/landsat-8 (accessed on 16 August 2018).
34. Key Hole Data. Available online: https://en.wikipedia.org/wiki/Key_Hole (accessed on 16 August 2018).
35. Introduction of SRTM 90 m Digital Elevation Data. Available online: http://srtm.csi.cgiar.org (accessed on 16 May 2018).
36. Crosetto, M.; Aragues, F.P. Radargrammetry and SAR interferometry for DEM generation: Validation and data fusion. In Proceedings of the CEOS'99 SAR Workshop ESA-CNES, Toulouse, France, 26–29 October 1999; pp. 367–372.
37. Ahmed, T.; Garg, A.; Singh, D.; Raman, B. An Approach to Monitor River Catchment with PALSAR Satellite Data. In Proceedings of the IEEE International Conference on Industrial and Information Systems, Gwalior, India, 15–17 December 2014; pp. 1–5.
38. Turcotte, R.; Fortin, J.P.; Rousseau, A.N.; Massicotte, S.; Villeneuve, J.-P. Determination of the drainage structure of a watershed using a digital elevation model and a digital river and lake network. *J. Hydrol.* **2001**, *240*, 225–242. [CrossRef]
39. Yan, Y.; Tang, J.; Pilesjö, P. A combined algorithm for automated drainage network extraction from Digital Elevation Models. *Hydrol. Process.* **2018**, *32*, 1322–1333. [CrossRef]
40. Chureesampant, K.; Susaki, J. Land cover classification using multi-temporal SAR data and optical data fusion with adaptive training sample selection. In Proceedings of the International Geoscience and Remote Sensing Symposium (IGARSS), Munich, Germany, 22–27 July 2012; pp. 6177–6180.
41. Song, G. Study on Groundwater Dependent Ecosystem and Ecological Mechanisms of Vegetation Succession in Desert Lake-Basin Region. Ph.D. Thesis, Chang'an University, Xi'an, China, 2012.
42. Xu, L.; Yu, X. Several questions of army farming of West Han Dynasty. *J. Northwest Norm. Univ.* **1985**, 37–43. [CrossRef]
43. Stein, M.A. *Serindia*; Chinese Academy of Social Sciences Institute of Archaeology Trans., Guangxi Normal University Press: Guangxi, China, 1998; Volume 5.
44. Xing, W.; Hou, Y. Research on the downstream changes of the Danghe river at the beginning of the 18th-20th Century. *West. Reg. Stud.* **2010**, *69–77*, 123–124. [CrossRef]
45. Zhao, W.; Ma, J.; He, J. Groundwater recharge and geochemical evolution in the Dunhuang basin of Danghe river, northwest China. *Arid. Land Geogr.* **2015**, *38*, 1133–1141. [CrossRef]
46. Feng, S. Evolution of Shule He river system. *J. Univ.* **1981**, 138–143. [CrossRef]
47. Zheng, B.; Cao, H. Investigation on the lakes and marshes in the basins of Shu-le river and Dang river between Han and Tang dynasties. *J. Lanzhou Univ.* **2013**, *41*. [CrossRef]
48. Zheng, B.; Cao, H. Environmental evolution of downstream area of Shu-le river between Han and Tang dynasties. *J. Dunhuang Stud.* **2012**. [CrossRef]
49. Zheng, B.; Cao, H. River changes and environmental evolution of Guazhou between late Tang and Five Dynasties. *J. Dunhuang Stud.* **2009**. [CrossRef]

50. Wang, M. Study on the Changes of River and Lake Water System of Shule River Basin in Qing Dynasty. Master's Thesis, Shaanxi Normal University, Shaanxi, China, 2010.
51. Cheng, Y.; Cheng, Z. Studies on relationship between runoff characteristics of Danghe river basin and climate change in recent 40 years. *China Water Resour.* **2015**, 52–55. [CrossRef]
52. Li, X.; Zhang, L.; Guo, H.; Fu, W.; Lu, L.; Qiu, Y.; Wang, X.; Jia, G. Space recognition of eco-environment global change response of arid and semi-arid region of the Silk Road Economic Belt. *Bull. Chin. Acad. Sci.* **2016**, *31*, 559–566. [CrossRef]